Springer

KSME

Journal of Mechanical Science and Technology 32 (2) (2018) 885~895
www.springerlink.com/content/1738-494x(Print)/1976-3824(Online)
DOI 10.1007/s12206-018-0139-8

Optimal cold sink temperature for thermoelectric dehumidifiers †

Joonoh Kim[1], Keunhwan Park[1,2], Duck-Gyu Lee[3], Young Soo Chang[4] and Ho-Young Kim[1,5,*]

[1]*Department of Mechanical and Aerospace Engineering, Seoul National University, Seoul 08826, Korea*
[2]*Institute of Advanced Machines and Design, Seoul National University, Seoul 08826, Korea*
[3]*Korea Institute of Machinery and Materials, Daejeon 34103, Korea*
[4]*School of Mechanical Engineering, Kookmin University, Seoul 02707, Korea*
[5]*Big Data Institute, Seoul National University, Seoul 08826, Korea*

(Manuscript Received March 19, 2017; Revised September 28, 2017; Accepted October 26, 2017)

Abstract

We propose an optimal cold sink temperature for thermoelectric dehumidifiers based on theoretical and experimental investigations. We show that the optimal condition is such that the latent heat absorption rate per unit power supplied to the dehumidifier is maximized. In consideration of the cooling ability of Peltier pellet and the heat exchange characteristics of the cold sink, we estimate the condensation rate as a function of the cold sink temperature. The theoretical predictions are compared with the results of experiments by using a prototype dehumidifier. We emphasize that the cold sink temperature is a critical parameter that determines the performance of dehumidification. Our study may provide an important insight to the thermoelectric dehumidification system and to designing a cold sink for thermoelectric dehumidifiers with improved energy efficiency.

Keywords: Cold sink; Condensation; Energy efficiency; Thermoelectric dehumidifier

1. Introduction

Reducing humidity is a critical task of air-conditioning system to maintain the quality of indoor air as comfortable and sanitary. Although vapor-compression type dehumidifiers have been widely used, thermoelectric dehumidifiers are recently on the rise due to their several advantages related to environmental issues [1]. Thermoelectric systems use the Peltier effect, by which heat flows from cold to hot sides as an electric current flows through the junctions of heterogeneous conductors in a thermoelectric pellet [2]. Water vapor is condensed on a solid surface contacting the cold side of the Peltier pellet while its hot side is cooled by external means to discharge the heat transferred by the Peltier effect. The latent heat of condensing vapor is absorbed by the cold side of the Peltier pellet, not by refrigerant that changes its phase in vapor-compression system [3]. As the mechanical parts associated with transport of refrigerant is missing in the thermoelectric system, most of the elements that compose the system are in solid state [4]. This feature causes less noise and vibration compared with the vapor-compression system [5]. Thus, the thermoelectric system requires less maintenance and can be more compact and light without a large compressor.

However, the low energy efficiency of the thermoelectric system has been a crucial problem that needs to be resolved [4, 6]. In other words, the heat absorption rate of the Peltier pellet is insufficient compared with the vapor-compression type system. In order to address this issue, many studies have been conducted to enhance the energy efficiency of thermoelectric systems.

A large number of researchers have endeavored to enhance the heat dissipation efficiency of the Peltier system. Udomsakdigool et al. [7] studied the heat sink performance of a rectangular fin array used for thermoelectric dehumidifiers. When the air flows parallel to the fin length direction, the optimum distance between the fan and the sink for the enhanced heat discharge rate was suggested. Thermal performance of the rectangular fin heat sink in impinging air flow was investigated by Li et al. [8]. The influence of the fin design parameters, such as impingement distance, width and height of the fins, and Reynolds number of the impinging flow on the heat exchange performance was studied by estimating thermal resistance of the fins by using the infrared thermography technique. Specific values of fin design parameters to enhance the heat exchange performance were suggested. Astrain et al. [9] developed a device called TSF for the heat dissipation from the Peltier pellet in a thermoelectric refrigerator based on the principle of phase change. Experiments with prototype refrig-

*Corresponding author. Tel.: +82 2 880 9286, Fax.: +82 2 880 9287
E-mail address: hyk@snu.ac.kr
† Recommended by Associate Editor Jae Dong Chung

erators proved that the use of TSF increases the coefficient of performance up to 32 % compared with systems with conventional fin dissipaters [10, 11]. Riffat et al. [12] also suggested a new method that can enhance the thermal performance of the heat sink in a thermoelectric refrigerator by using an encapsulated phase change material in place of the conventional heat sink, and demonstrated improved performance by using prototype refrigerators. A microchannel heat sink for a thermoelectric cooler was suggested [13], and the thermal performance of the heat sink was investigated by a theoretical model based on a lumped system and the experimental analysis. They reported that the minimum temperature of the refrigerated object can be achieved by decreasing thermal resistance of the heat sink, and presented the design parameters for minimum thermal resistance of the sink.

Some of the related studies focused on the operating parameters of thermoelectric systems. Chen et al. [14] investigated the heat transfer rate and thermal efficiency of thermoelectric cooling systems for air conditioning applications, and revealed that inconsistent current distribution should be used for obtaining maximum efficiency of the thermoelectric cooling system with a heat exchanger. Vián et al. [15] optimized the electric voltage supplied to the Peltier pellet and fans in low power thermoelectric dehumidifiers by a computational model and the numerous experiments with a prototype dehumidifier. The COP of the dehumidifier was estimated with various voltage conditions, and the optimum values were presented. Huajun et al. [16] and Hua et al. [17] revealed that typical thermoelectric dehumidifiers experience two thermodynamic processes and presented the optimum input power that maximizes the operation performance of a low power thermoelectric cooling dehumidifier by experimental investigations. They argued that rapid elimination of liquid drops condensed on the cold sink is an important issue for improving the performance of thermoelectric dehumidifiers. Alaoui et al. [18] studied the performance of a Peltier pellet based refrigerator with the change of supplied power, and proposed the appropriate range of the input power that maximizes the COP.

Most of the aforementioned researches have aimed at improving heat discharge performance of the heat sink in thermoelectric systems. However, in thermoelectric dehumidifiers, the highest heat discharge rate of the Peltier pellet would not guarantee the highest latent heat absorption rate which determines the COP of dehumidification systems. With the increase of the cold sink temperature, total heat absorption rate of the Peltier pellet increases but the contribution of the latent heat to the total heat absorption rate decreases. Hence, the cold sink temperature plays an important role in determining the latent heat absorption rate, and the optimum value should be considered prior to other operating parameters when designing the thermoelectric dehumidification system. Therefore, we investigate the effects of the cold sink temperature on the latent heat absorption rate of thermoelectric dehumidifiers in the following.

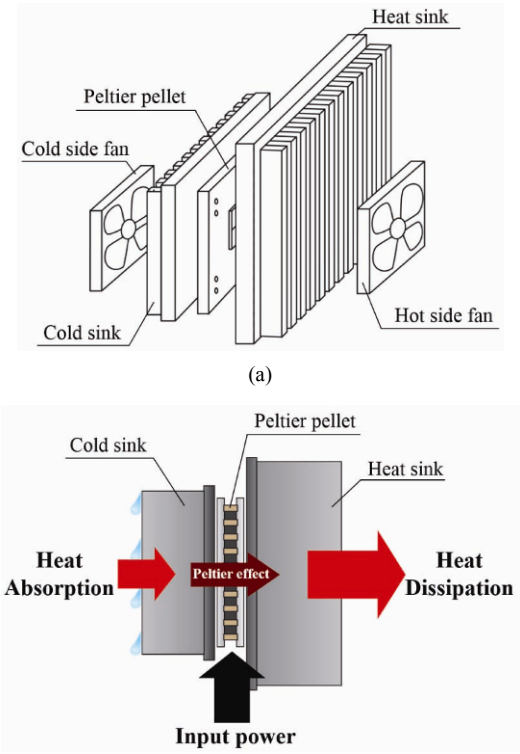

Fig. 1. Structure and heat transfer model of a thermoelectric dehumidification system: (a) Structure of a thermoelectric dehumidification unit; (b) schematic diagram of heat flow through a thermoelectric dehumidification system.

2. Analysis of heat flow in thermoelectric dehumidifiers

2.1 Heat transfer in thermoelectric dehumidifiers

A thermoelectric dehumidifier consists of three parts: A Peltier pellet, a cold sink, and a heat sink [15]. On either side of the Peltier pellet, the cold and heat sinks exchange heat with ambient air, as shown in Fig. 1(a). When electric power is supplied to the Peltier pellet, heat absorption occurs through the cold sink while heat dissipation occurs through the heat sink as depicted in Fig. 1(b).

The heat dissipation rate corresponds to the sum of supplied electric power and the heat absorption rate by the energy conservation. The heat absorbed through the cold sink has two components [19]: The heat transferred by convection resulting from the temperature difference between the cold sink and ambient air, and the latent heat released by water vapor condensing around the cold sink. When the constant power is supplied to the dehumidification system, maximizing the absorbed latent heat should increase dehumidification efficiency.

2.2 Total heat absorption rate and ratio of latent heat to total heat absorption

To increase the latent heat transfer rate, two quantities should be considered: The total heat absorbed through the cold

sink and the ratio of latent heat contributing to the total heat absorption. The total heat absorption is determined by the heat absorption rate of the Peltier module and the heat exchange rate of the cold sink. The heat absorption rate of the Peltier module is determined by the combined effect of the following three heat transfer modes [20-22]: The heat conveyed by the Peltier effect in proportion to the temperature difference of the cold and hot sides, the heat generated by the conduction resulting from the temperature gradient within the Peltier pellet, and the Joule heating due to the current flow through the resistor in the electric circuit. Hence, the heat absorption rate of the Peltier module is expressed as follows [22]:

$$q_a = (T_c + 273)\alpha_m I - (T_h - T_c)K_m - \frac{1}{2}I^2 R_m . \quad (1)$$

The heat dissipation rate is also determined by the combined effect of the three aforementioned components [22]:

$$q_d = (T_h + 273)\alpha_m I - (T_h - T_c)K_m + \frac{1}{2}I^2 R_m . \quad (2)$$

R_m, α_m, K_m, are the electrical resistance, Seebeck coefficient and thermal conductivity of the Peltier pellet, respectively, and each coefficient can be calculated by the following equations [21, 22]:

$$R_m = \frac{V_{max}((T_\infty + 273) - \Delta T_{max})}{I_{max}(T_\infty + 273)} \quad (3)$$

$$\alpha_m = \frac{V_{max}}{T_\infty + 273} \quad (4)$$

$$K_m = \frac{I_{max}V_{max}((T_\infty + 273) - \Delta T_{max})}{2\Delta T_{max}(T_\infty + 273)} . \quad (5)$$

Here, ΔT_{max}, V_{max}, and I_{max} are the characteristic specifications of the Peltier pellet, and T_∞ is the temperature of ambient air flowing into the cold and heat sinks. The heat exchange rate of the cold sink depends on the two heat transfer rates caused by convection and condensation [19, 23]:

$$q_e = q_v + q_L \quad (6)$$

where q_v is the convective heat transfer rate in the humid air:

$$q_v = A_c h_c (T_\infty - T_c) . \quad (7)$$

q_L is the heat liberation rate on the cold sink surface due to condensation:

$$q_L = \rho_a h_m A_c i_{fg} (\omega_\infty - \omega_c) . \quad (8)$$

Since the Lewis number defined as Le = α/D is near unity for air and water vapor mixtures, Eq. (8) can be written as [19, 23, 24]:

$$q_L = A_c h_c \frac{i_{fg}}{c_p}(\omega_\infty - \omega_c) . \quad (9)$$

Thus, from Eqs. (6), (7) and (9), the heat exchange rate of the cold sink is expressed as:

$$q_e = A_c h_c [(T_\infty - T_c) + \frac{i_{fg}}{c_p}(\omega_\infty - \omega_c)] . \quad (10)$$

In Eq. (10), the humidity ratio of saturated air at T_c is given by a polynomial expression obtained from the regression analysis for the temperature range ($0 \le T_c \le 30$) [19, 25]:

$$\omega_c = (3.7444 + 0.3078T_c + 0.0046T_c^2 + 0.0004T_c^3) \times 10^{-3} . \quad (11)$$

The specific latent heat of water condensation is expressed as a function of the cold sink temperature [26]:

$$i_{fg} = (2500.8 - 2.36T_c + 0.0016T_c^2 - 0.00006T_c^3) \times 10^3 . \quad (12)$$

At the beginning of heat absorption, the cold sink temperature is nearly the same as the ambient temperature, and the heat absorption rate of the Peltier module and the heat exchange rate of the cold sink cannot be balanced. With time, the two rates converge to a balance point, and the heat absorption system is in a steady state, resulting in a constant cold sink temperature [7, 15] and a constant total heat absorption rate through the cold sink. The total heat absorption rate is obtained in accordance with Eq. (1) at each cold sink temperature. In Eq. (1), when we use the same Peltier pellet with supplying the same electric power, as the heat sink temperature is maintained at almost constant, the total heat absorption rate can be considered a function of the cold sink temperature. A detailed description of this functional relation is in Sec. 2.3.

To maximize the latent heat transfer rate, we should consider the ratio of the latent heat that contributes to the total heat absorption rate. As the total heat absorption rate is determined by the balance of the heat absorption rate of the Peltier module and the heat exchange rate of the cold sink, the ratio of the latent heat is expressed as follows from Eq. (10):

$$\frac{q_L}{q_c} = \frac{\frac{i_{fg}}{c_p}(\omega_\infty - \omega_c)}{\frac{i_{fg}}{c_p}(\omega_\infty - \omega_c) + (T_\infty - T_c)} . \quad (13)$$

In Eq. (13), $(T_\infty - T_c)$ represents the sensible heat absorption rate, and $(i_{fg}/c_p)(\omega_\infty - \omega_c)$ represents the latent heat absorption rate. We define $(T_\infty - T_c)$ and $(i_{fg}/c_p)(\omega_\infty - \omega_c)$ as the sensible term

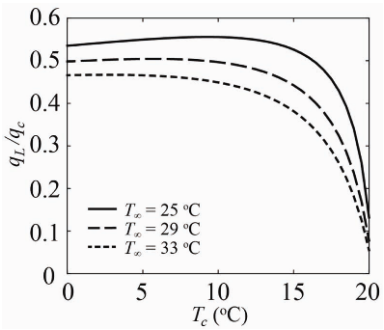

(a)

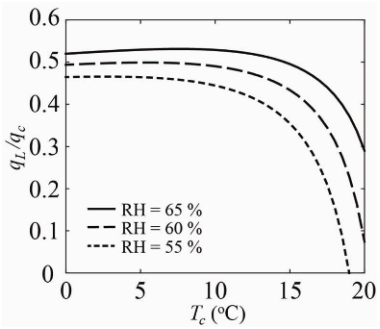

(b)

Fig. 2. Ratio of the latent heat to the total heat absorption rate as a function of the cold sink temperature for different ambient temperature and relative humidity conditions: (a) Ratio of the latent heat to the total heat absorption with variation of ambient temperature when the ambient specific humidity is fixed as 0.01502 kg/kg; (b) ratio of the latent heat to the total heat absorption with variation of ambient relative humidity when the ambient temperature is fixed as 29 °C.

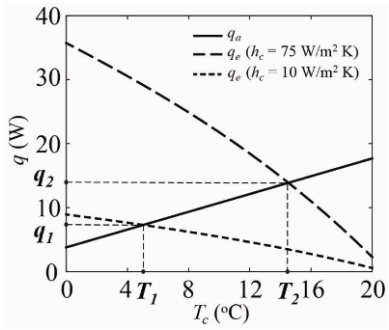

(a)

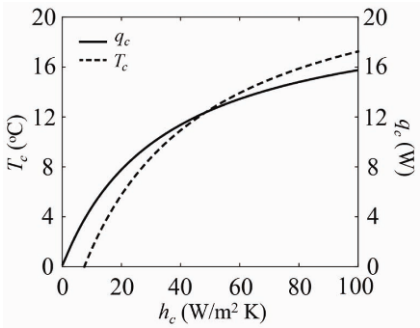

(b)

Fig. 3. Change of the cold sink temperature and the total heat absorption rate with the heat transfer coefficient of the cold side. Ambient temperature and ambient relative humidity, and the power supplied to the dehumidifier are held constant at 29 °C, 60.3 % and 39.74 W, respectively. I_{max}, V_{max} and ΔT_{max} are held as 6.3 A, 27.7 V and 78 °C, respectively: (a) Change of the intersection point where the heat absorption rate of Peltier pellet (Solid line) and the heat exchange rate of the cold sink (Short and long dashed lines) are balanced. T_1 is the cold sink temperature and q_1 is the heat absorption rate at low heat transfer of 10 W/m^2 K. T_2 and q_2 are the cold sink temperature and the heat absorption rate, respectively, at relatively high heat transfer of 75 W/m^2 K; (b) variation of the cold sink temperature and the total heat absorption rate.

and the latent term, respectively. The sensible term is a temperature difference between ambient air and the cold sink surface. In the latent term, c_p and i_{fg} are nearly constant in usual dehumidification systems. Thus, the latent term is dominantly determined by (ω_∞-ω_c) which is the difference between the humidity ratio of ambient air and the saturated humidity ratio of air near the cold sink surface. With increase of the cold sink temperature, the temperature difference and the humidity ratio difference decrease. When the cold sink temperature is low, as the reduction rate of temperature difference and that of the humidity ratio difference are comparable, the portion of the latent heat in the total heat absorption rate is nearly constant as in Fig. 2(a). However, when the cold sink temperature increases beyond a certain value, approximately 11 °C in Fig. 2(a) in the 29 °C ambient temperature condition, the ratio of latent heat drastically decreases as the reduction rate of the humidity difference becomes larger than that of the temperature difference. The latent heat ratio decreases regardless of the ambient conditions, and the cold sink temperature that the latent heat ratio begins to drastically decrease varies depending on ambient conditions. In conclusion, to maximize the latent heat transfer rate, the total heat absorption rate and latent heat ratio should be taken into consideration simultaneously, both of which are functions of the cold sink temperature.

2.3 The optimal cold sink temperature

The cold sink temperature and the total heat absorption rate are determined by the balance of two performances: Heat exchange rate of the cold sink and heat absorption rate of the Peltier pellet as stated in Sec. 2.2. As shown in Fig. 3(a), when the heat transfer coefficient of the cold side increases, the balance point of the two performances changes with the increase of the cold sink temperature and the heat absorption rate. The short-dashed line in Fig. 3(a) corresponds to the heat exchange rate of the cold sink as a function of the cold sink temperature in Eq. (10) when the heat transfer coefficient of the cold side is approximately 10 W/m^2 K. The solid line in Fig. 3(a) is the heat absorption rate of the Peltier pellet in Eq. (1) when such factors as heat sink temperature, ambient conditions, and power supplied are constant. It linearly increases with the cold sink temperature due to the decrease of conduction loss in the Peltier pellet. The slope of the short-dashed line increases with the heat transfer coefficient of the cold side [8, 27]. The long-dashed line in Fig. 3(a) corresponds to the heat exchange rate

of the cold sink when the heat transfer coefficient of the cold side is approximately 75 W/m^2 K. The solid line is not affected by the change of the heat transfer condition, i.e. the heat transfer coefficient. As a result, the intersection point of the two heat transfer rates moves upward to the right along the solid line as the heat transfer coefficient increases, which means that the resultant cold sink temperature and the total heat absorption rate both determined at the intersection point increase. Fig. 3(b) shows that the heat absorption rate and the cold sink temperature increase simultaneously as the heat transfer coefficient of the cold sink increases. Practically, when the condition of the heat transfer changes, the solid line moves because the heat sink temperature changes with the heat absorption rate. However, the solid line is nearly consistent because the heat sink temperature variation is very small. As the contribution of consistent electric power to the heat dissipation rate is fairly large, the heat absorption rate hardly affects the heat dissipation rate. Hence, the heat sink temperature, which is determined by the heat dissipation rate, can be assumed to be nearly consistent.

Meanwhile, the latent heat ratio decreases when the cold sink temperature excessively increases, as stated in Sec. 2.2. There exists an optimal cold sink temperature that balances this trade-off that the total heat absorption rate increases but the latent heat ratio decreases with increase of the cold sink temperature. Therefore, it is necessary to operate thermoelectric dehumidifiers under the optimal operating condition, especially for the cold sink temperature, in order to remove water vapor in air with maximum energy efficiency.

3. Analytical model for predicting the condensation rate of thermoelectric dehumidification systems

We have theoretically calculated the condensation rate which is proportional to the latent heat absorption rate at various cold sink temperatures. In dehumidification systems, the cold sink temperature changes along with various heat transfer conditions, electric power supplied to the Peltier pellet, and the ambient air temperature and humidity. Here, we have focused on the effects of the heat transfer coefficient of the cold side, as it is the most practical parameter that we can change to examine the effect of the cold sink temperature. We have calculated the condensation rate in the following procedure.

We first calculate the steady cold and heat sink temperatures. The following two equations determine the sink temperatures at steady state. The first is the balance between the heat exchange rate of the cold sink and the heat absorption rate of the Peltier pellet:

$$A_c h_c[(T_\infty - T_c) + \frac{i_{fg}}{c_p}(\omega_\infty - \omega_c)] = (T_c + 273)\alpha_m I - (T_h - T_c)K_m - \frac{1}{2}I^2 R_m \,. \quad (14)$$

The other equation states the balance between the heat exchange rate of the heat sink and the heat dissipation rate of the Peltier pellet:

$$A_h h_h (T_h - T_\infty) = (T_h + 273)\alpha_m I - (T_h - T_c)K_m + \frac{1}{2}I^2 R_m \,. \quad (15)$$

The two equations are coupled through the two variables: the cold and heat sink temperatures. We deduce the sink temperatures by simultaneously solving the two equations. Then, we calculate the steady total heat absorption rate and the latent heat absorption rate which are the functions of the cold sink temperature as described in Sec. 2.2. The amount of water condensed on the cold sink can be determined as a term proportional to the heat transfer rate caused by the phase change. It is expressed as follows [23]:

$$\dot{m}_w = \frac{A_c h_c}{c_p}(\omega_\infty - \omega_c) = \frac{q_L}{i_{fg}} \,. \quad (16)$$

When we apply various heat transfer coefficients of the cold sink to the foregoing procedures as inputs, the cold sink temperature and the condensation rate are sequentially calculated under each heat transfer condition. We have used the cold side heat transfer coefficient with increasing at regular intervals within a specific range. We have specified the variation range of heat transfer coefficient as a similar condition to condensation experiment. Approximate scale of the heat transfer coefficient in the experiments have been estimated by using the fact that sensible heat loss of air flowing through the cold sink can be considered to be equal to the sensible heat exchange rate between air and the cold sink:

$$\dot{m}_{a,c} c_p (T_{i,c} - T_{o,c}) = h_c A_c (T_\infty - T_c) \,. \quad (17)$$

The left-hand side of Eq. (17) can be calculated by measuring the mass flow rate and the temperatures of air at the inlet and outlet of the cold side. In the right-hand side of Eq. (17), as the temperatures of ambient air and the cold sink can be measured in the experiments, the heat transfer coefficient can be estimated. Under the condition where the temperature of ambient air, relative humidity, and the power supplied to the dehumidifier are held constant as 29 °C, 57 % and 39.74 W, respectively, the cold side heat transfer coefficient is estimated as 28.8 W/m^2 K when the cold sink temperature is obtained as 8.6 ^{o}C. On the 17 ^{o}C cold sink temperature case, the heat transfer coefficient is estimated as 101.3 W/m^2 K. From these experimental estimations, we have varied the heat transfer coefficient from 8 W/m^2 K to 205 W/m^2 K with the constant increment of 0.5 W/m^2 K. When substituting this range of the cold side heat transfer coefficient into our theoretical model, we can obtain the cold sink temperature whose range is approximately from 0 ^{o}C to 20 ^{o}C. With change of the ambient condition, we have altered the variation range of the cold side heat transfer coefficient to obtain enough cold sink tempera-

ture conditions to find out the tendency of condensation rate change. We have compared the h_c values in the theoretical prediction and in the experiments on each cold sink temperature condition, and we have identified that the values of h_c in the theoretical prediction are similar to the h_c estimated in experiments on each condition.

In our theoretical model, the optimal temperature that maximizes the condensation rate is deduced to be about 14 °C under the condition where the temperature of ambient air, relative humidity, and the power supplied to the dehumidifier are held constant at 29 °C, 57 % and 39.74 W, respectively.

4. Experimental setup and method

The condensation rate was measured by using a prototype dehumidifier shown in Fig. 4. The specifications of the Peltier pellet and the fins used in the device are presented in Tables 1 and 2. Two fans are installed in the dehumidifier to blow air through acrylic ducts for heat exchange at each sink. When the humid air contacts the cold sink, water vapor condenses on the cold sink because the temperature of the sink is lower than the dewing point. The condensed water falls into the container placed beyond the cold sink owing to gravity. After an hour of each experiment, we measured the mass of the container including water dropped from the cold sink by using the scale, and the condensation rate was obtained by subtracting the mass of the container from the measured value. To alter the cold sink temperature, we varied the airflow velocity toward the cold sink by controlling the electric power input to the fan. The thermometers were embedded at the bottom of each fin, and the temperatures of the cold sink and heat sink were measured in real-time. As the height of the fins is considerably short with 1 cm of the cold sink and 2 cm of the heat sink, the temperature difference along the height direction is very small as less than 1 °C, and this is verified by the experiment that measured the temperature gradient along the fins. Thus, the temperature difference between the top and bottom of the fins can be negligible. The mass flow rate of air toward each sink was obtained by measuring air velocity at regular intervals, 1.5 cm for the cold sink and 3 cm for the heat sink, in the fin exit, and the average velocity was used to estimate the mass flow rate. The temperature of the air flowing out of each sink was obtained by measuring temperatures at regular intervals, 1.5 cm for the cold sink and 3 cm for the heat sink, in the fin exit, and the average temperature was used. The aforementioned parameters were recorded in each experimental case.

Table 1. Specifications of thermoelectric (Peltier) pellet used in the prototype dehumidifier.

Specifications		Characteristics
Model		HMN 6055 MCS
Maximum current		6.3 A
Maximum voltage		27.7 V
Maximum cooling power		105 W
Maximum temperature difference		78 °C
Electrical resistance		4.0 Ω (at 25 °C)
Width		55 ± 0.6 mm
Length		55 ± 0.6 mm
Height		4.0 ± 0.2 mm
Wire length	Red	300 ± 10 mm
	Black	300 ± 10 mm

Table 2. Specifications of the cold side and hot side finned heat exchangers.

Fins	Characteristics	
Finned cold sink	Material	Aluminum
	Base area	50 mm × 40 mm
	Fin height	10 mm
	Fin thickness	1.5 mm
	Space between fins	4 mm
Finned heat sink	Material	Aluminum
	Base area	127 mm × 180 mm
	Fin height	21 mm
	Fin thickness	1 mm
	Space between fins	3.5 mm

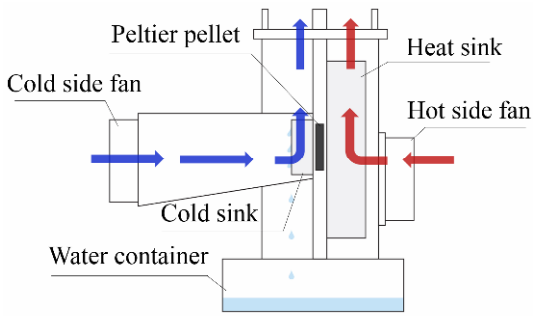

Fig. 4. Schematic of the prototype thermoelectric dehumidifier.

5. Results and discussions

5.1 Energy balance analysis

We have verified the energy balance of the prototype dehumidifier to confirm the reliability of the experiments. As stated in Sec. 2.1, the amount of the heat dissipated through the heat sink is equivalent to the sum of the heat absorption rate of the cold sink and the electric power supplied to the Peltier pellet [20, 21]. Eq. (18) describes this balance in the dehumidification system:

$$q_h = q_c + P_T \,. \tag{18}$$

The terms in Eq. (18) can be expressed as follows:

$$q_h = \dot{m}_{a,h}\, c_p (T_{o,h} - T_{i,h}) \tag{19}$$

$$q_c = \dot{m}_{a,c}\, c_p (T_{i,c} - T_{o,c}) + i_{fg}\dot{m}_w \tag{20}$$

$$P_T = IV \,. \tag{21}$$

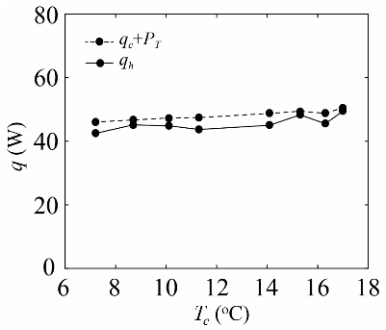

Fig. 5. Results of the energy balance test at various cold sink temperatures. The energy delivered to the prototype (Dashed line) and the energy discharged from the system (Solid line) are shown for comparison.

The heat dissipation and absorption rate through the sinks and the electric power supplied to the Peltier pellet are calculated with Eqs. (19)-(21) by substituting the values measured in each experiment. Therefore, the heat dissipation rate can be compared to the sum of the heat absorption rate and the electric power in order to verify the energy balance of the prototype system. The energy balance test have been conducted on eight cold sink temperature cases under the condition where the temperature of ambient air, relative humidity, and the power supplied to the dehumidifier are held constant as 29 °C, 57 % and 39.74 W, respectively. As shown in Fig. 5, the energies that delivered to and discharged from the system have a similar tendency in that both slightly increase as the cold sink temperature increases. The maximum difference between the two energies is approximately 6.4 W, which is about 12.6 % of the energy delivered to the system, when the cold sink temperature is 11.3 °C. The minimum difference is approximately 2.1 W, which is about 4.5 % of the energy delivered to the system at the cold sink temperature of 7.2 °C.

One reason behind this discrepancy is that there exists additional heat dissipation through the lateral side of the Peltier pellet. In the Peltier pellet, three heat transfer modes occur: The heat conveyed by the Peltier effect, the heat generated by conduction and the Joule heating due to the current flow. Although the heat flow due to the Peltier effect and conduction occurs from front to rear side or rear to front side of the Peltier pellet, the heat caused by Joule heating is transmitted in all directions. However, we assume that all the heat from the Joule heating flows toward front or rear side, not the lateral side of the Peltier pellet. In Sec. 5.1, we only consider the heat transfer rates through the front and rear side of the Peltier pellet as in Eqs. (19) and (20).

Also, the loss of energy at the wire that connects the power supply and the Peltier pellet must have caused the errors. We estimate the electric energy applied to the prototype dehumidifier as the product of the applied current and voltage which are displayed on power supply. However, there exists some power loss in a 1.5 m long wire connecting the power supply and the prototype dehumidifier, which means that the supplied electric power in Fig. 5 is overestimated.

5.2 Condensation rate variations with the cold sink temperature

To find the optimal temperature of the cold sink, we measured the condensation rate in response to changes in the cold sink temperature. The characteristics of the electric power input to the fans, flow velocities, and sink temperatures are presented in Table 3. We measured the condensation rates of these eight cases of cold sink temperatures and compared the results with the theoretical model. To find the optimal condition that maximizes energy efficiency, the supplied electric power was controlled to be constant as 39.74 W by the power supplier connected to the Peltier pellet with wires. We consistently maintained atmospheric conditions in the programmable temperature and humidity chamber. Due to the large volume of the chamber, there exists gradient of the air conditions. As the prototype dehumidifier removes water vapor, the humidity ratio of air around the system is somewhat lower than the set values of the chamber. In addition, the disturbance caused by the air flowing through the dehumidification system and the control error of the programmable chamber result in fluctuations of the ambient conditions. The average ambient conditions which we measured at near the prototype dehumidifier were 29 °C of temperature and 57 % of relative humidity.

Fig. 6(a) presents the experimental and theoretical results for condensation rate variations with cold sink temperatures. The theoretical prediction of the condensation rate is made in the 57 % ambient relative humidity condition. Reflecting the fluctuations in the ambient relative humidity, we also have plotted theoretical graphs on 55.5 % and 58.5 % relative humidity condition which is the lower and upper bound of fluctuation. The fluctuation of ambient temperature is not reflected in the theoretical prediction due to small variation of the temperature compared to the change of the humidity. In experiment, the maximum condensation rate is obtained when the cold sink temperature is 15.3 °C, which is similar to the theoretical result of 14 °C. This result shows that the thermoelectric dehumidifier absorbs the maximum latent heat when the cold sink temperature is approximately 15.3 °C. Under our experimental condition, the maximum water condensation rate is about 7.6 g/h. The errors have been presented by indicating the error bars in Fig. 6(a) which have been estimated by calculating the standard deviation of the measurements.

As shown in Fig. 6(a), the most of the experimental results are at near the condensation rate predicted by our theoretical model on 57 % relative humidity condition of ambient air. However, there exists some discrepancy between the theoretical prediction on 57 % relative humidity condition and experimental results, and as the cold sink temperature increases, the difference becomes larger. We discuss the reasons of this difference in the following.

First, the fact that we estimate the condensation rate by measuring the amount of water gathered in the container below the cold sink may bring about the errors. After the experiment, droplets which have not fallen to the container still remains on

Table 3. Properties of the fans and fin temperatures in each experimental case.

Cold sink fan		Heat sink fan		Cold side inlet air velocity (m/s)	Hot side inlet air velocity (m/s)	Cold sink temperature (°C)	Heat sink temperature (°C)
I (A)	*V* (V)	*I* (A)	*V* (V)				
0.02	3.9	0.05	5.2	0.14	0.23	7.2	48.9
0.03	4	0.05	5.2	0.29	0.23	8.6	49.2
0.05	5.3	0.05	5.2	0.41	0.23	10.1	49.8
0.05	5.6	0.05	5.2	0.50	0.23	11.3	50.1
0.09	9	0.05	5.2	0.96	0.23	14.1	50.7
0.12	11.8	0.05	5.2	1.46	0.23	15.3	50.8
0.22	18.6	0.05	5.2	2.29	0.23	16.3	50.8
0.26	23.9	0.05	5.2	2.74	0.23	17	50.8

the cold sink surface. Besides, as the water gathered in the container is exposed to the air flowing through the cold side, some of the water may evaporate to the air. However, we start the experiment after the cold sink surface is completely covered by water film and the additionally condensed water is continuously falling off. Thus, the amount of water left on the cold sink surface after the experiment can be considered the same as the water which existed before we start the experiment. Besides, as the exposed area of the collected water is narrow in the container, the evaporation rate is very small compared to the total condensation rate. Therefore, the remaining water on the cold sink after experiment and the evaporation rate of gathered water have a minor influence on the error in Fig. 6(a).

Meanwhile, the ambient conditions of air near the dehumidification system fluctuates during the experiment, which would bring about the discrepancy in Fig. 6(a). As the programmable chamber controls the temperature and humidity conditions of inner air from the feedback of measuring the conditions in the chamber, the air conditions would fluctuate. When the ambient conditions change, the cold sink temperature which is determined by coupling the two equations, Eqs. (14) and (15), is perturbed. Also, with change of ambient conditions, the latent heat ratio contributing to the total heat absorption rate changes as in Fig. 2, which brings about the different condensation rate even on the same cold sink temperature condition. As in the theoretical prediction depicted in Fig. 6(a), in the high cold sink temperature range, the variation of ambient relative humidity has more influence on the change of condensation rate than on the low cold sink temperature condition. In addition, in the high cold sink temperature condition, the velocity of air flowing through the cold sink is faster than on the low temperature range, which causes greater disturbance of ambient conditions. Thus, the possibility that the errors of condensation rate occur would increase on the high cold sink temperature condition.

In Fig. 6(b), we present the COP estimated based on the condensation rate data at each cold sink temperature condi tion. COP of the thermoelectric dehumidification system is defined as follows:

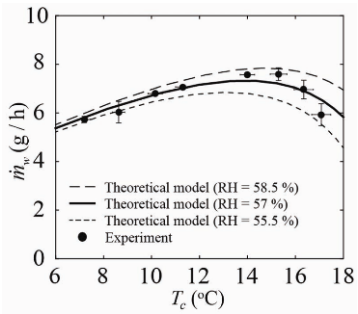

(a)

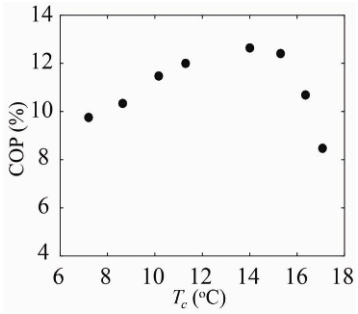

(b)

Fig. 6. Condensation rate and COP at various cold sink temperatures: (a) Theoretical predictions and experimental results of condensation rate at various cold sink temperatures; (b) experimentally estimated COP of thermoelectric dehumidifier at various cold sink temperatures.

$$\mathrm{COP} = \frac{q_L}{P_T + P_F}. \tag{22}$$

The COP's have a similar tendency with the condensation rates in Fig. 6(a), and the maximum COP is achieved when the cold sink temperature is 14.1 °C. As the electric power supplied to the Peltier pellet is fairly larger than the power supplied to the fans, the COP is mainly depedent on the condensation rate which is proportional to the latent heat absorption rate. Despite the largest condensation rate, COP on 15.3 °C cold sink temperature condition is nearly lower than 14.1 °C condition, due to the larger electric power supplied to the cold side fan.

5.3 Condensation rate variations depending on atmospheric conditions

Changes in atmospheric conditions would cause variations in the optimal cold sink temperature as the heat exchange rate of the fins is altered. The changes in the optimal cold sink temperature are estimated using the theoretical model described in Sec. 3. We measured the condensation rate under two cold sink temperature cases for each ambient condition. The supplied electric power was controlled to be constant as 39.74 W. The results of the theoretical prediction and experiments are depicted in Fig. 7.

In Fig. 7(a), the condensation rate variations with the cold

sink temperature are depicted under two ambient temperature conditions when the specific humidity is fixed as 57 % of saturated humidity ratio at 29 °C of ambient temperature. The decrease of the ambient temperature leads to the increase of the latent heat ratio as shown in Fig. 2(a). It results in the higher condensation rate and slightly higher optimal temperature. In Fig. 7(b), the condensation rate is depicted under two relative humidity conditions at 29 °C of ambient temperature. The increase of ambient relative humidity leads to an increase in the latent heat ratio as shown in Fig. 2(b), which causes the higher condensation rate. Meanwhile, as the cold sink temperature increases, the difference of condensation rate with variation of the ambient relative humidity becomes larger in Fig. 7(b). When the cold sink temperature is 7 °C, the difference of condensation rate between the 55 % and 65 % relative humidity conditions is 1.1 g/h, but the difference becomes approximately 3.5 g/h when the cold sink temperature is 15 °C. The total heat absorption rate through the cold sink is identical regardless of the relative humidity condition as dictated in Eq. (1). However, the latent heat ratio changes under each relative humidity condition as shown in Fig. 2(b). When comparing the 55 % and 65 % relative humidity conditions, the cold sink temperature that the latent heat ratio starts to steeply decrease is slightly lower on 55 % relative humidity condition. It causes the difference of latent heat ratio between the two relative humidity conditions to become larger with increase of the cold sink temperature. When the cold sink temperature is 7 °C, the difference of latent heat ratio between the two conditions is 0.07, but the difference is predicted to be 0.16 when the cold sink temperature is 15 °C. As the total heat absorption rate linearly increases with the cold sink temperature as in Eq. (1), even the small difference of the latent heat ratio between the two conditions brings about large difference of the latent heat absorption at high cold sink temperature, leading to the large difference of the condensation rate. Thus, the difference of condensation rate by change of the relative humidity conditions becomes larger as the cold sink temperature increases, and the optimal temperature increases with the ambient relative humidity. As shown in Fig. 7, the effect of relative humidity on the optimal temperature is more dominant than that of the temperature.

The experimental results are very similar with the theoretical predictions. The discrepancy between the experimental and theoretical results is larger at high cold sink temperature condition. It is because the condensation rate is more influenced by fluctuations in ambient conditions on high cold sink temperature conditions as described in Sec. 5.2.

5.4 Theoretical prediction of the condensation rate variations depending on specifications of the Peltier pellet

We have estimated the condensation rate with change of ΔT_{max}, the maximum temperature difference between the cold and hot sides of the Peltier pellet without any external load such as forced flow of ambient air. This parameter implies the heat transfer performance of the Peltier pellet. As depicted in Fig. 8(a), more vapor is condensed on the cold sink surface with the increase of ΔT_{max}, which is attributed to the enhanced heat absorption performance of the Peltier pellet. In Fig. 8(b), the optimal cold sink temperature decreases with the ΔT_{max}. When ΔT_{max} increases, the balance point of the heat absorption rate of the Peltier pellet and the heat exchange rate of the cold sink is determined at the lower cold sink temperature to obtain the same total heat absorption rate, which causes the cold sink temperature maximizing the condensation rate, in Fig. 8(a), to decrease. Hence, the optimal temperature decreases.

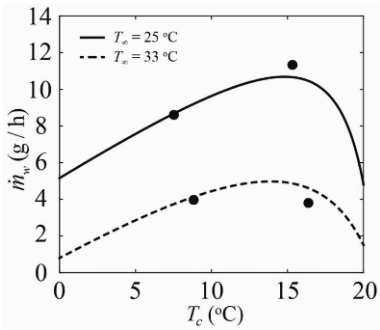

(a)

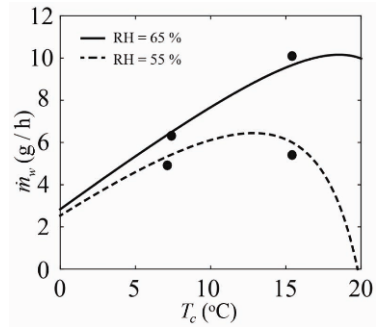

(b)

Fig. 7. Theoretical predictions and experimental results of condensation rate with change of the cold sink temperature for various ambient temperature and relative humidity conditions: (a) Condensation rate versus cold sink surface temperature with change of ambient temperature; (b) condensation rate versus cold sink temperature with change of ambient relative humidity.

6. Conclusions

We have introduced the method to identify the optimum cold sink temperature for thermoelectric dehumidifiers. By analyzing the heat flow in the Peltier module, we have found that the optimum cold sink temperature exists that maximizes the latent heat absorption rate of a thermoelectric dehumidifier. Our theoretical model can calculate the condensation rate which is proportional to the latent heat absorption rate at various cold sink temperatures, and thus deduce the optimum temperature as 14 °C. This theoretical optimum temperature has been verified through experiments with the prototype dehumidifier. When the atmospheric temperature is 29 °C and

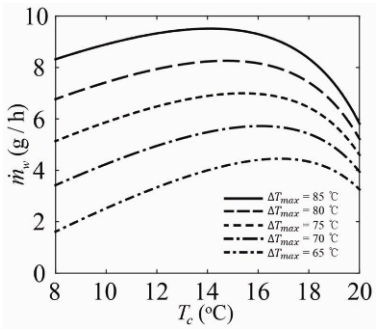

(a)

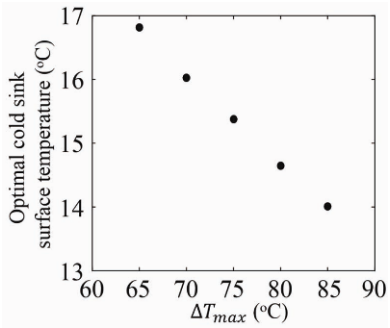

(b)

Fig. 8. Condensation rate and optimal cold sink temperature with variation of ΔT_{max}. Ambient temperature and ambient relative humidity, and the power supplied to the dehumidifier are held constant at 29 °C, 60.3 % and 39.74 W, respectively. I_{max} and V_{max} are held as 6.3 A and 27.7 V, respectively: (a) Condensation rate as a function of cold sink temperature with variation of ΔT_{max}; (b) optimal cold sink temperature as a function of ΔT_{max}.

the relative humidity is 57 %, the optimum cold sink temperature for maximizing condensation rate is approximately 15.3 °C, and the cold sink temperature for maximizing COP is 14.1 °C. We have predicted variations in the optimal cold sink temperature with different atmospheric conditions by using the theoretical model. As the ambient temperature decreases and the relative humidity increases, the optimum temperature and the condensation rate increase. The relative humidity influences the condensation rate more severely than the ambient temperature. The variation of the optimal cold sink temperature with the change of Peltier specification has also been theoretically predicted. When ΔT_{max} of a Peltier pellet increases, more vapor is condensed and the optimal cold sink temperature decreases. The model we have proposed here will allow for operation of thermoelectric dehumidifiers under the optimal condition that improves the dehumidification energy efficiency of the system.

Acknowledgments

This work was supported by Ministry of Trade, Industry and Energy (Technology Innovation Program, 10038702) and National Research Foundation of Korea (Grant nos. 2016901290 and 2016913167).

Nomenclature

A_c : Heat transfer area of the cold sink (m^2)
A_h : Heat transfer area of the heat sink (m^2)
COP : Coefficient of performance
c_p : Specific heat of dry air at constant pressure (J/kg K)
D : Diffusion coefficient (m^2/s)
h_c : Convective heat transfer coefficient of the cold side (W/m^2 K)
h_h : Convective heat transfer coefficient of the hot side (W/m^2 K)
h_m : Mass transfer coefficient (m/s)
I : Current through the thermoelectric pellet (A)
I_{max} : Maximum electric current (A)
i_{fg} : Specific latent heat of condensation (J/kg)
K_m : Total thermal conductivity of Peltier module (W/K)
k : Thermal conductivity (W/m K)
Le : Lewis number defined as α/D
$\dot{m}_{a,c}$: Mass flow rate of air that flows through the cold sink (kg/s)
$\dot{m}_{a,h}$: Mass flow rate of air that flows through the heat sink (kg/s)
$\dot{m}_w$: Mass flow rate of condensation (g/h)
P_F : Electric power supplied to the fans at the cold and hot sides (W)
P_T : Electric power supplied to the thermoelectric pellet (W)
q_a : Heat absorption rate of the Peltier pellet (W)
q_c : Total heat transfer rate through the cold sink at steady state (W)
q_d : Heat dissipation rate of the Peltier pellet (W)
q_e : Heat exchange rate of the cold sink with ambient air (W)
q_h : Heat transfer rate through the heat sink at steady state (W)
q_L : Latent heat absorbed through the cold side (W)
q_v : Sensible heat absorbed through the cold side (W)
R_m : Total electrical resistance of Peltier module (Ω)
RH : Ambient relative humidity (%)
T_c : Cold sink surface temperature (°C)
T_h : Heat sink surface temperature (°C)
$T_{i,c}$: Temperature of air at the inlet of the cold sink (°C)
$T_{i,h}$: Temperature of air at the inlet of the heat sink (°C)
$T_{o,c}$: Temperature of air at the outlet of the cold sink (°C)
$T_{o,h}$: Temperature of air at the outlet of the heat sink (°C)
T_∞ : Ambient temperature (°C)
V : Voltage to the thermoelectric pellet (V)
V_{max} : Maximum electric voltage (V)
α : Thermal diffusivity defined as $k / \rho_a c_p$ (m^2/s)
α_m : Seebeck coefficient of Peltier module (V/K)
ΔT_{max} : Maximum temperature difference (°C)
ρ_a : Density of air (kg/m^3)
ω_c : Humidity ratio of saturated air at T_c (kg/kg)
ω_∞ : Humidity ratio of ambient air (kg/kg)

References

[1] D. M. Rowe, Thermoelectrics, an environmentally-friendly

source of electrical power, *Renew. Energy*, 16 (1-4) (1999) 1251-1256.
[2] S. B. Riffat and X. Ma, Improving the coefficient of performance of thermoelectric cooling systems: A review, *Int. J. Energy Res.,* 28 (9) (2004) 753-768.
[3] S. B. Riffat and G. Qiu, Comparative investigation of thermoelectric air-conditioners versus vapour compression and absorption air-conditioners, *Appl. Therm. Eng.*, 24 (14) (2004) 1979-1993.
[4] K. Manohar and A. A. Adeyanju, Comparison of the experimental performance of a thermoelectric refrigerator with a vapour compression refrigerator, *International Journal of Technical Research and Applications*, 2 (3) (2014) 1-5.
[5] S. B. Riffat and X. Ma, Thermoelectrics: a review of present and potential applications, *Appl. Therm. Eng.*, 23 (8) (2003) 913-935.
[6] P. K. Bansal and A. Martin, Comparative study of vapour compression, thermoelectric and absorption refrigerators, *Int. J. Energy Res.*, 24 (2) (2000) 93-107.
[7] C. Udomsakdigool, J. Hirunlabh, J. Khedari and B. Zeghmati, Design optimization of a new hot heat sink with a re-ctangular fin array for thermoelectric dehumidifiers, *Heat Transfer Eng.*, 28 (7) (2007) 645-655.
[8] H.-Y. Li and K.-Y. Chen, Thermal performance of plate-fin heat sinks under confined impinging jet conditions, *Int. J. Heat Mass Transfer*, 50 (9) (2007) 1963-1970.
[9] D. Astrain, J. G. Vián and M. Domínguez, Increase of COP in the thermoelectric refrigeration by the optimization of heat dissipation, *Appl. Therm. Eng.*, 23 (17) (2003) 2183-2200.
[10] J. G. Vián and D. Astrain, Development of a heat exchanger for the cold side of a thermoelectric module, *Appl. Therm. Eng.*, 28 (11) (2008) 1514-1521.
[11] J. G. Vián and D. Astrain, Optimisation of a thermosyphon used to dissipate heat from a Peltier pellet, Domestic refrigeration application, *J. Thermoelectr.,* 2 (2001) 55-68.
[12] S. B. Riffat, S. A. Omer and X. Ma, A novel thermoelectric refrigeration system employing heat pipes and a phase change material: an experimental investigation, *Renew. Energy,* 23 (2) (2001) 313-323.
[13] R. Chein and Y. Chen, Performances of thermoelectric cooler integrated with microchannel heat sinks, *Int. J. Refrig.*, 28 (6) (2005) 828-839.
[14] K. Chen, An analysis of the heat transfer rate and efficiency of TE (thermoelectric) cooling systems, *Int. J. Energy Res.*, 20 (5) (1996) 399-417.
[15] J. G. Vián, D. Astrain and M. Domínguez, Numerical modelling and a design of a thermoelectric dehumidifier, *Appl. Therm. Eng.*, 22 (4) (2002) 407-422.
[16] W. Huajun and Q. Chengying, Experimental study of operation performance of a low power thermoelectric cooling dehumidifier, *Int. J. Energy Environ.*, 1 (3) (2010) 459-466.
[17] Y. Hua, Z. Kang and Q. Chengying, Experimental investigation of operation characteristics of a thermoelectric dehumidifier, *3rd International Conference on Knowledge Discovery and Data Mining,* IEEE (2010) 163-166.
[18] C. Alaoui and Z. M. Salameh, Solid state heater cooler: Design and evaluation, *Power Engineering. Large Engineering Systems Conference on. IEEE* (2001) 139-145.
[19] A. Lee, M.-W. Moon, H. Lim, W.-D. Kim and H.-Y. Kim, Water harvest via dewing, *Langmuir*, 28 (27) (2012) 10183-10191.
[20] J. A. Chávez, J. A. Ortega, J. Salazar, A. Turó and M. J. García, SPICE model of thermoelectric elements including thermal effects, *Proc. of the 17th IEEE Instrumentation and Measurement Technology Conference*, 2 (2000) 1019-1023.
[21] C. Alaoui, Peltier thermoelectric modules modeling and evaluation, *Int. J. Eng.*, 5 (1) (2011) 114.
[22] S. Lineykin and S. Ben-Yaakov, Modeling and analysis of thermoelectric modules, *IEEE Trans. Ind. Appl.*, 43 (2) (2007) 505-512.
[23] J. E. R. Coney, C. G. W. Sheppard and E. A. M. El-Shafei, Fin performance with condensation from humid air: A numerical investigation, *Int. J. Heat Fluid Flow*, 10 (3) (1989) 224-231.
[24] ASHRAE Handbook, *Fundamentals 2005*, American Society of Heating, Refrigerating and Air Conditioning Engineers, Atlanta, USA (2005).
[25] B. Kundu, Approximate analytic solution for performances of wet fins with a polynomial relationship between humidity ratio and temperature, *Int. J. Therm. Sci.*, 48 (11) (2009) 2108-2118.
[26] R. R. Rogers and M. K. Yau, *A short course in cloud physics*, Third Ed., Butterworth-Heinemann Press (1989).
[27] G. Comini, C. Nonino and S. Savino, Numerical evaluation of fin performance under dehumidifying conditions, *J. Heat Transfer*, 129 (10) (2007) 1395-1402.

Joonoh Kim received his B.S. degree from Korea University in mechanical engineering. He is currently a Ph.D. candidate in the Department of Mechanical Engineering at Seoul National University. His research interests include multiphase flows and spray dynamics.

Keunhwan Park received his B.S. and Ph.D. degrees from Seoul National University all in mechanical engineering. He is now a postdoc of physics at Technical University of Denmark. His research activities involve the domains of biological physics, evolutionary biology, cell biology, fluid dynamics and applied mathematics.

Ho-Young Kim received his B.S. degree from Seoul National University and M.S. and Ph.D. degrees from MIT all in mechanical engineering. He is now a Professor of mechanical engineering at Seoul National University. His research activities revolve around microfluid mechanics, biomimetics, and soft matter physics.